The most popular name of Chlorophytum Borivilianum in India is Safed Musli. The various parts of the Chlorophytum Borivilianum plant contain medicinal property; however, the most utilized part for above mentioned application is roots. Roots of Chlorophytum Borivilianum are an important ingredient of several Ayurvedic and Unani drugs. The roots are also used as a sex tonic for curing sexual weakness of humans. Chlorophytum Borivilianum roots, Liliaceae family, contain numerous bioorganic compounds, such as, Flavonoids, Saponins, Tannins and carbohydrates [Kenjale et al., 2007]. These compounds are rich in heteroatoms and aromatic rings, which meets with the fundamental requirements of a corrosion inhibitor. Hence, we have selected Chlorophytum roots for corrosion inhibition studies.

4.1 Characterization of Chlorophytum Borivilianum Root Extract (CBRE)

HPLC Study:

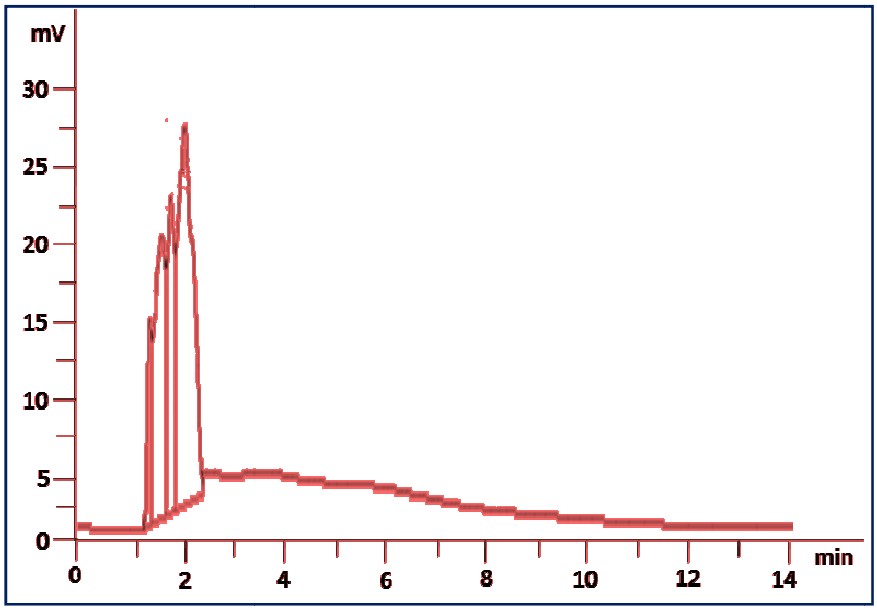

Figure 4.1 HPLC Chromatograph of aqueous extract of Chlorophytum Borivilianum root

Figure 27 illustrates HPLC chromatogram of aqueous root extract of Chlorophytum Borivilianum root extract. It is evident from Figure that peak 4 is the major constituent of the extract followed by 2, 3 and 1 among detected compounds of the extract. However, we have not identified the compounds separately because a lot of work has been done on Chlorophytum Borivilianum roots, which have confirmed the strong presence of Saponins in the roots.

FTIR and UV-Visible Spectroscopy:

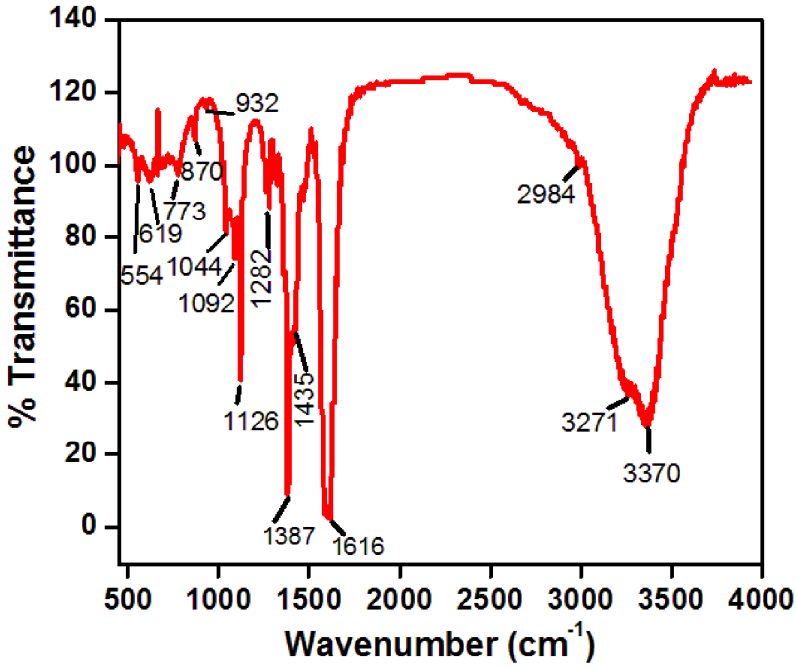

Figure 4.2 FTIR spectrum of aqueous root extract of *Chlorophytum Borivilianum*

Figure 28 shows FT-IR spectrum of Chlorophytum Borivilianum Root Extract. A strong and broad peak is observed at 3370 cm^{-1}, which can be assigned to N-H or O-H stretching frequencies. An absorption band at 3271 cm^{-1} can be related to N-H stretching of the primary amines. A small peak at 2984 cm^{-1} is noticed due to C-H stretching frequency. A strong absorption band at 1616 cm^{-1} can be attributed to C=C and C=N stretching, or N-H

bending vibration frequency. A small peak at 1435 cm^{-1} indicates O-H bending vibration. A strong peak at 1387 cm^{-1} is associated with CH_3 or C-H in plane bending vibration. There are 4 small peaks in the range of 1000 cm^{-1} to 1300 cm^{-1}, which correspond to C-N or C-O stretching frequency. The absorption bands below 1000 cm^{-1} indicate presence of aliphatic and aromatic C-H functional groups. Thus, on the basis of FT-IR study it can be concluded that *Chlorophytum Borivilianum* aqueous root extract contains the chemical compounds that have C-N, C-O, O-H, N-H, C=N linkages as well as aromatic rings in various functional groups.

It has been previously reported that furostanol saponins show characteristic IR peaks in the frequency range of 1600 -1700 $cm^{-1}$and 3350-3400 cm^{-1} [Deore et al, 2010]. With the support of this fact, we can say that furostanol saponins are present in the extract since strong peaks are observed at 3370 cm^{-1} and 1616 cm^{-1} (Figure 28).

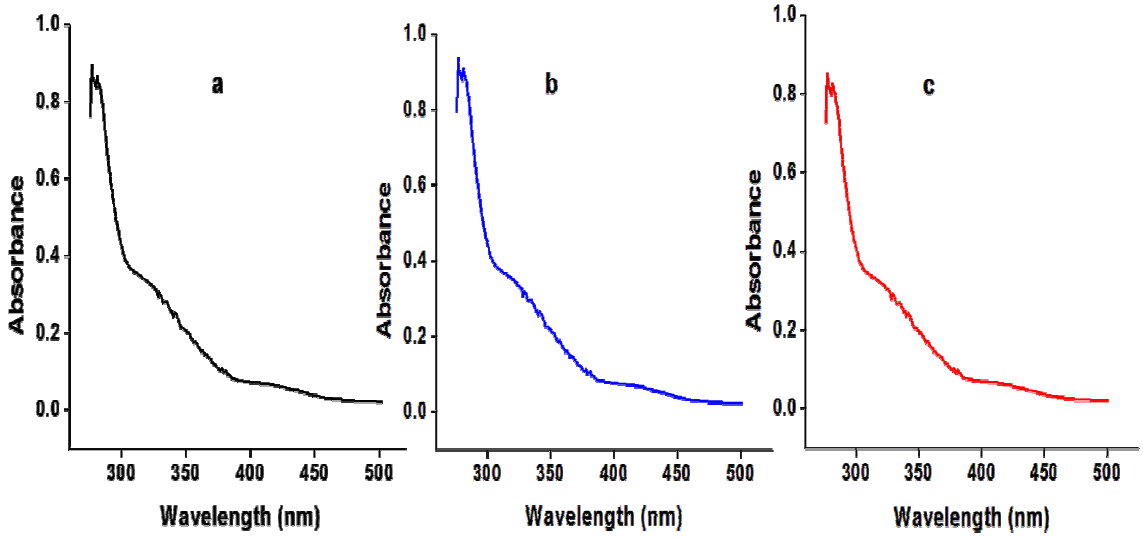

Figure 4.3 Uv-visible spectra of a) the pure extract, b) 500 mg L^{-1} of extract in 1 M HCl solution and c) 500 mg L^{-1} extract in 0.5 M H_2SO_4 solution

Figure 29 illustrates Uv-Visible spectrum of the pure extract as well as the solutions containing washings of the mild steel samples immersed in HCl and H_2SO_4 media with 500 mg L^{-1} of CBRE. Careful inspection of Figure 29 revealed that the spectrum shows similar peaks in absorption curves; however, intensity of the peaks was altered. This fact suggested that the chemical constituents of CBRE were successfully adsorbed on the mild steel surface. Furthermore, two sharp bands could be clearly observed at 275 and 280 nm in the spectra of the extract as well as some small peaks appeared in the range of 300-400 nm, indicating that aromatic compounds were present in the extract [Kamal et al., 2012; Ouchrif et al., 2005].

4.2 Weight Loss Measurements

Figure 30 shows effect of CBRE concentration on inhibition efficiency and corrosion rate in HCl and H_2SO_4 solutions. From inspection of the results, as shown in Figure 30, it was revealed that heavy loss in the weights of specimens occurred on immersion in acid solutions. However, effective corrosion inhibition was acknowledged in presence of CBRE in both acid media. Further, investigation of Figure 30 provided that corrosion resistance of mild steel drastically increased with the concentration of CBRE and achieved a maximum value at 500 mg L^{-1} inhibitor concentration in both acid solutions. On addition of 500 mg L^{-1} of the extract corrosion rate effectively lowered from 36.30 to 3.10 mmpy and from 42.80 to 7.2 mmpy in 1 M HCl and 0.5 M H_2SO_4 (Figure 30a) respectively. Exhibiting similar behavior, inhibition efficiency increased with inhibitor concentration with a maximum value of 90% in HCl and 83 % in H_2SO_4 (Figure 30b). The effective corrosion inhibition of mild steel in corrosive solutions could be attributed to significant blocking of the reactive sites on the surface by the extract molecules. With

increase in inhibitor concentration, the effective surface area was decreased due to enhanced activity of adsorbed inhibitor molecules. However, no significant effect of CBRE was observed beyond 500 mg L^{-1} inhibitor concentration.

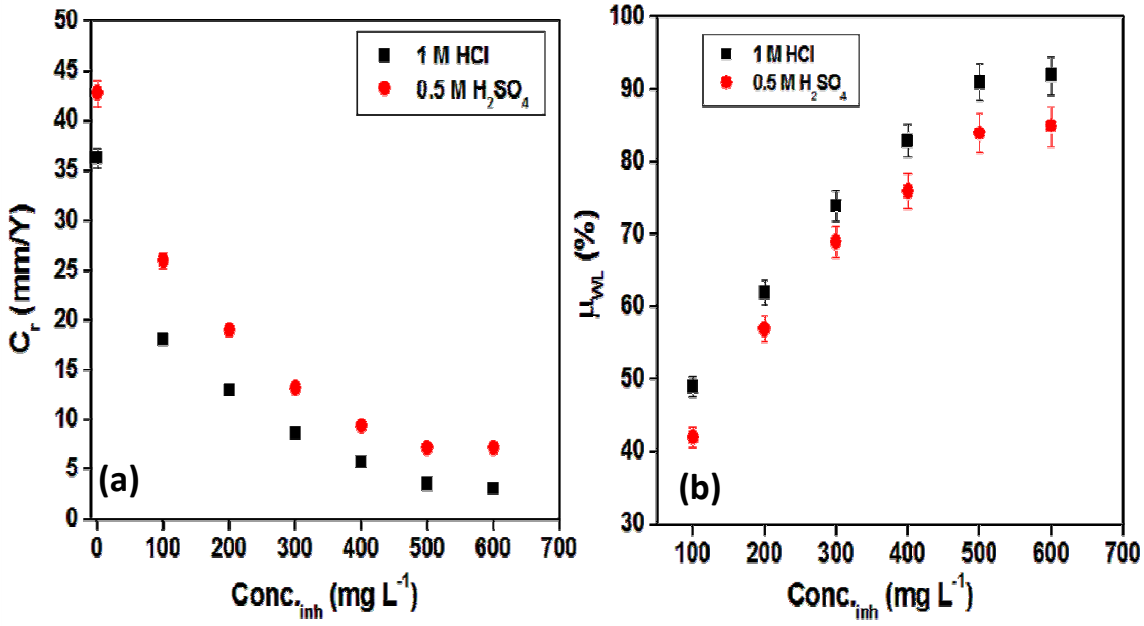

Figure 4.4 Showing (a) Corrosion rate and (b) Inhibition efficiency obtained at different concentrations of CBRE in 1 M HCl and 0.5 M H_2SO_4 at 26±1° C for 5h.

4.2.1. Adsorption Study

To know the adsorption behavior of CBRE in acid media, adsorption isotherms were employed to analyze the results of weight loss measurements. There are many isotherm models that are used to describe adsorption of inhibitors over metals, such as, Langmuir, Temkin, Frumkin, Flory-Huggins, Freundlich and El-awady. The efforts were directed towards fitting of the results according to various adsorption isotherms. But, we found the best results for Langmuir isotherm in both acid solutions. Langmuir isotherm relates surface coverage θ to concentration of inhibitor C by the relation described in Equation 15. The various parameters were calculated from the curves and listed in Table 7.

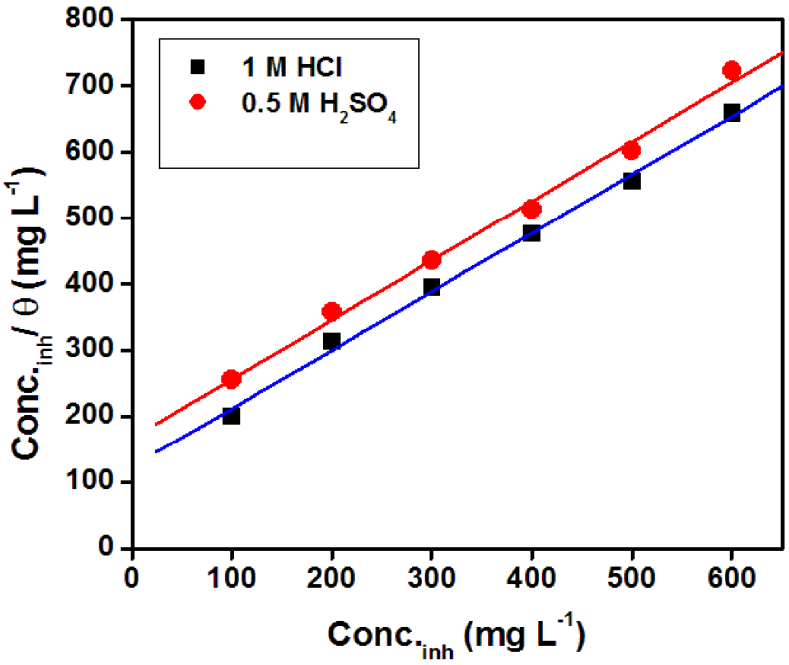

Figure 4.5 Langmuir isotherm fitting for mild steel in 1 M HCl and 0.5 M H_2SO_4 containing different concentrations of inhibitor.

Table 4.1 Various parameters obtained from straight lines drawn between C/θ and C.

Corrosive medium	Slope	Intercept (g L^{-1})	K_{ads} (L g^{-1})
1 M HCL	0.910	0.118	8.50
0.5 M H_2SO_4	0.902	0.172	5.81

A graph between C/θ and concentration of inhibitor C was plotted on the basis of weight loss data (Figure 31), which was found in accordance with Langmuir isotherm. A high values of regression coefficient (R^2= 0.9984 and 0.9972) were obtained in both the cases. In addition, the slopes of the fitting curves were very close to one suggesting that Langmuir isotherm was the most suitable candidate among all the studied isotherms. Furthermore, higher value of K_{ads} (8.50 L g^{-1}) was recognized in 1 M HCl than the value

(5.81 L g^{-1}) in 0.5 M H_2SO_4, indicating that CBRE was more effectively adsorbed over mild steel surface in hydrochloric acid than sulfuric acid.

4.2.2 Effect of Immersion Time

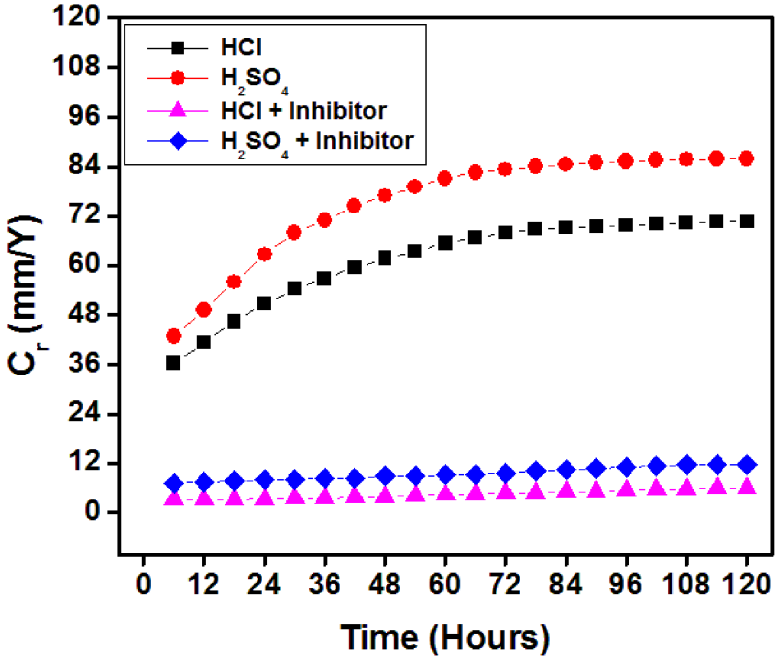

Figure 4.6 Showing effect of immersion time on inhibition potential (500 mg L^{-1}) of the extract in 1 M HCl and 0.5 M H_2SO_4 at 26±1° C for 120 Hours

The effect of immersion time on inhibitive performance of CBRE (500 mg L^{-1}) was investigated in 1 M HCl and 0.5 M H_2SO_4 at 26±1° C for 120 hours. It is apparent from Figure 32 that corrosion rate in blank acid solutions drastically increased to 78 hours and retained almost constant value for rest of the immersion time. Initially (6 Hours), corrosion rate was 36.3 and 42.8 mmpy in 1 M HCl and 0.5 M H_2SO_4 respectively, which was surprisingly increased to 70.6 mmpy (HCl) and 86 mmpy (H_2SO_4) at the end of the experiment. However, corrosion rate slightly changed in the presence of CBRE suggesting that inhibitor molecules were highly stable in acidic environment. After 6 hours corrosion rate was 3.1 and 7.2 mmpy in 1 M HCl and 0.5 M H_2SO_4

correspondingly, while it was 5.60 mmpy (HCl) and 11.7 mmpy (H_2SO_4) after 120 hours. Increased resistance of mild steel against aggressive attack of acid solutions could be accredited to the high stability of the extract molecules, which acted as an inhibitive barrier for corroding molecules and efficiently reduced exposure area of metal surface in acid media for long time [Bentiss et al., 2005, Bentrah et al., 2014]. However, a slight increase in corrosion rate values occurred with time. This might be happened due to disintegration of inhibitor molecules, which exposed larger surface area for corrosion [A.K. Singh 2012].

4.2.3 Effect of Acid Concentration on Corrosion Inhibition

Figure 33 demonstrates change in inhibition efficiency and corrosion rate values of 500 mg L^{-1} CBRE with acid concentration. Careful inspection of Figure 33a revealed that corrosion rate of mild steel in HCl slowly increased up to 3 M, but increased at a faster rate for further increase in acid concentration. In contrast, inhibition efficiency diminished at slower rate to 3 M HCl while significant acceleration in reduction was observed for higher concentration of HCl. Similar changes were observed in H_2SO_4 solutions (Figure 33b). In any case it was noticed that higher inhibition potential of CBRE was achieved in hydrochloric acid than sulfuric acid. The retarded inhibition effect of CBRE with increase in concentration of both acid media could be ascribed to higher desorption rate of inhibitor molecules from the metal-acid interface [Mathur and Vasudevan, 1982]. It was also possible that adsorption rate of CBRE from solution to metal surface was inhibited by higher content of acid molecules, which caused lowering in inhibitive effect of the extract [Moretti et al., 2013].

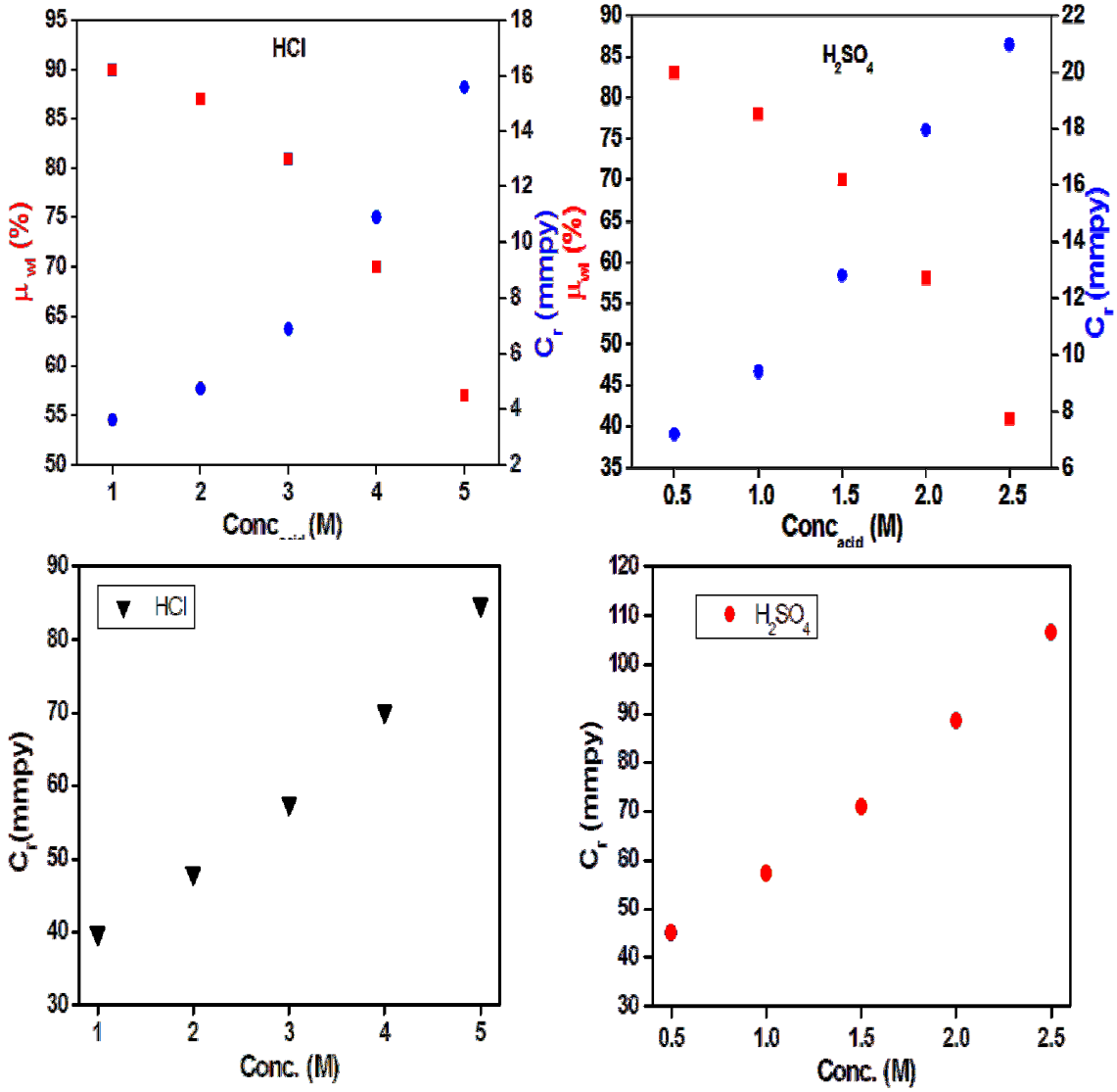

Figure 4.7 Inhibition efficiencies and corrosion rates for 500 mg L^{-1} CBRE in different concentration of (a) HCl (b) H_2SO_4 solutions and in blank acid solutions.

4.2.4 Effect of Temperature on Corrosion Inhibition

Figure 34 illustrates the effect of temperature (30˚-60˚ C) on inhibitive performance of CBRE in 1 M HCl and 0.5 M H_2SO_4. Careful inspection of Figure 34 revealed that slope and intercept values of straight lines increased with the extract concentration in both acid solutions, indicating that the energy of activation and Arrhenius coefficient value accelerated HCl and H_2SO_4 solutions in presence of Chlorophytum Borivilianum extract.

This observation revealed that the extract molecules physically adsorbed on mild steel surface; however, larger values of activation energy and Arrhenius constant were acknowledged in hydrochloric acid than sulfuric acid solution [Pournazari et al., 2013]. The same fact was reflected from the corrosion parameters shown in Table 8. Thus, it could be concluded from above discussion that addition of inhibitor raised the energy limit of protective barrier for corrosive molecules and retarded mild steel corrosion in acid media [Sorkhabi et al., 2005].

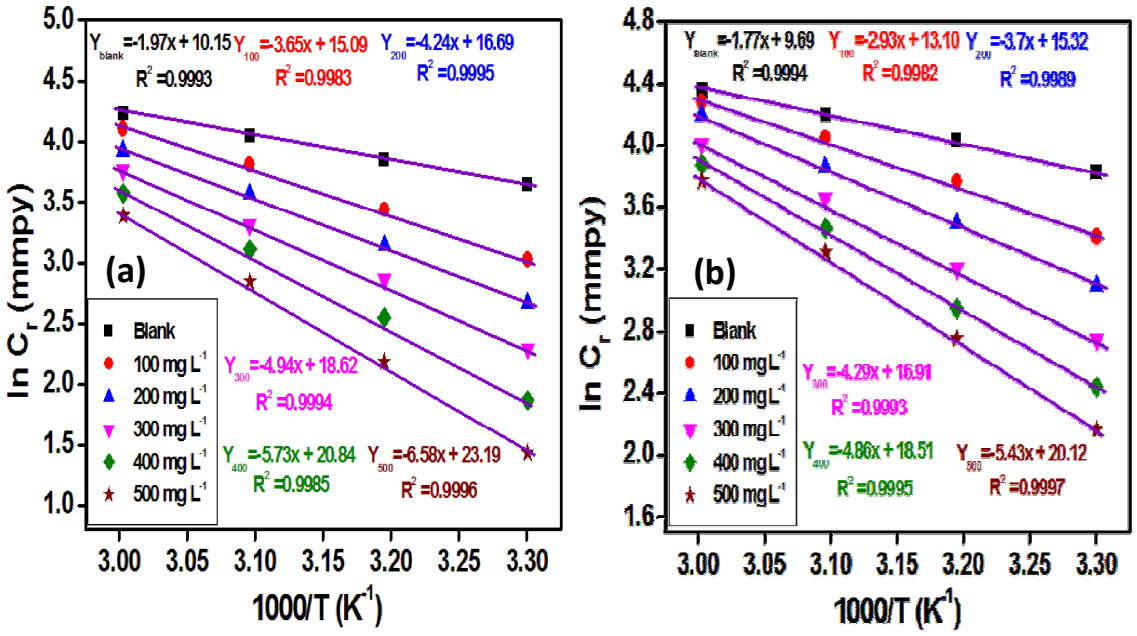

Figure 4.8 Arrhenius plot for mild steel in (a) 1 M HCl and (b) 0.5 M H_2SO_4 with different concentrations of CBRE

Figure 35 shows the straight line fitting between C_r/T and 1/T values obtained for mild steel in HCl and H_2SO_4 solutions. The values of change in enthalpy (ΔH^*) of activation and entropy (ΔS^*) of activation were calculated by Transition state equation (Eq. 19) and mentioned in Table 8. Analysis of Table 8 and Figure 35 revealed that the ΔH^* values of inhibited mild steel were greater than the values of uninhibited sample. In addition, ΔH^* values were positive at different concentrations of the extract. The above mentioned facts

suggested that the value of minimum energy for mild steel corrosion enhanced with the CBRE concentration, which made it difficult for acid solutions to corrode metal in presence of inhibitor [Mu et al., 2004, Lecante et al., 2011]. The greater values of ΔH^* in HCl than values in H_2SO_4 indicated that the extract performed more efficiently in hydrochloric acid. Furthermore, it could be clearly observed from Table 8 that there was a well known relation (Eq. 22) between ΔH^* and E_a in both acid media, which validated the experimental results of thermodynamic experiments.

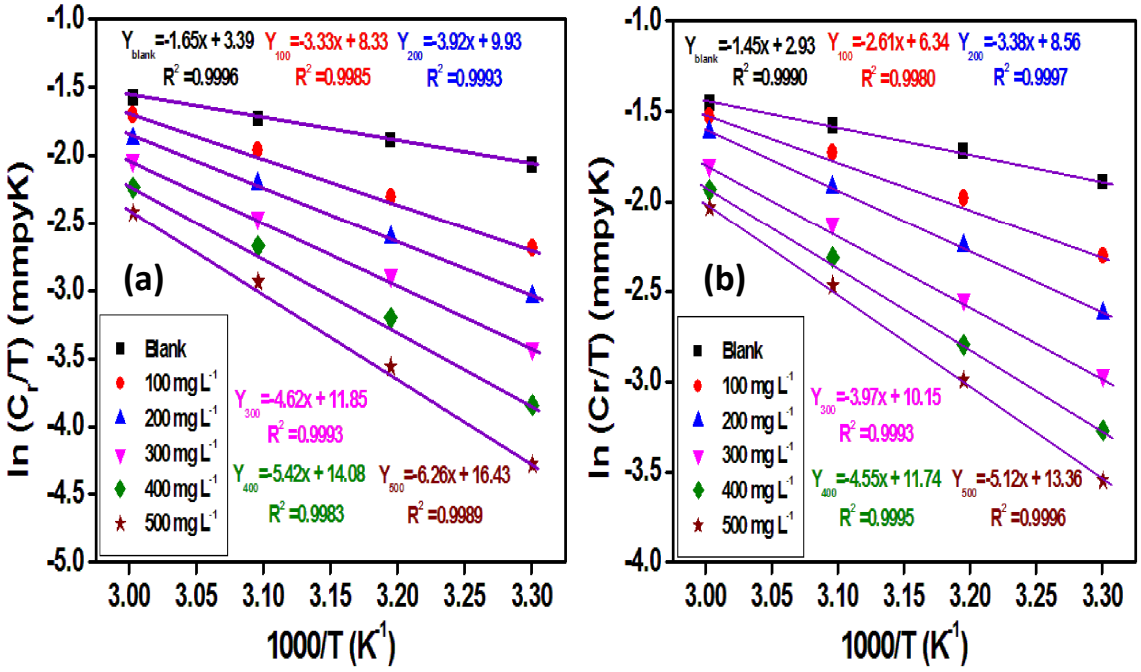

Figure 4.9 Transition state plots for mild steel in (a) 1 M HCl and (b) 0.5 M H_2SO_4 with different concentrations of CBRE

Through inspection of ΔS^* values listed in Table 8, it was observed that randomness of the system increased as a function of the extract concentration. Probably, the reactants were converted into activated complex as the reactions proceeded, which might occur due to molecular adsorption of the extract over mild steel surface [Sahin et al., 2002, Pereira et al., 2012]. In aqueous solutions, the adsorption of the organic moieties on metals can

be considered as quasi-substitution reactions between water and inhibitor molecules. On this basis, it could be stated that the extract molecules substituted water molecules from the metal surface during corrosion inhibition process. Accordingly, entropy of activation increased with CBRE concentration because of increase in entropy of the solvent. Furthermore, the greater values of ΔS^* in HCl than H_2SO_4 solution indicated that the effect of inhibitor on mild steel corrosion was more pronounced in hydrochloric acid with respect to sulfuric acid.

Table 4.2 Activation parameters for mild steel in 1 M HCl without and with different concentrations of CBRE

Acid solution	Conc. of Inhibitor (mg L^{-1})	A (mmpy)	Ea (kJ mol^{-1})	Δ H* (kJ mol^{-1})	ΔS* (J mol^{-1} K^{-1})	E_a- ΔH* (kJ mol^{-1})
HCl	Blank	2.67×10^4	16.37	13.71	-169.35	2.66
	100	3.81×10^6	30.34	27.68	-128.28	2.66
	200	1.9×10^7	35.25	32.59	-114.90	2.66
	300	1.32×10^8	41.07	38.41	-99.01	2.66
	400	1.22×10^9	47.65	45.00	-80.47	2.65
	500	1.30×10^{10}	54.70	52.04	-60.94	2.66
H_2SO_4	Blank	1.68×10^4	14.71	12.05	-173.18	2.66
	100	5.17×10^5	24.36	21.69	-144.82	2.67
	200	4.80×10^6	30.76	28.10	-126.37	2.66
	300	2.37×10^8	35.66	33.00	-113.16	2.66
	400	1.18×10^8	40.50	37.83	-99.93	2.67
	500	5.96×10^8	45.16	42.50	-86.46	2.66

4.3 Tafel Polarization Curves

Figure 36 illustrates polarization curves for mild steel in acid solutions with different concentrations of CBRE at 26±1° C. Careful inspection of Figure 36 revealed that inhibitor retarded corrosion current in a concentration dependent manner. The minimum corrosion current was obtained for 500 mg L^{-1} extract concentration. It could be observed from Tafel polarization curves that both anodic and cathodic corrosion reactions were diminished by CBRE (Figure 36); however, the extract had more pronounced effect on anodic reactions (mild steel dissolution) than cathodic reactions. The electrochemical parameters of Tafel polarization, such as, equilibrium corrosion potential (E_{corr}), corrosion current density (I_{corr}), anodic Tafel slope (b_a) and cathodic Tafel slope (b_c) are determined and listed in Table 9.

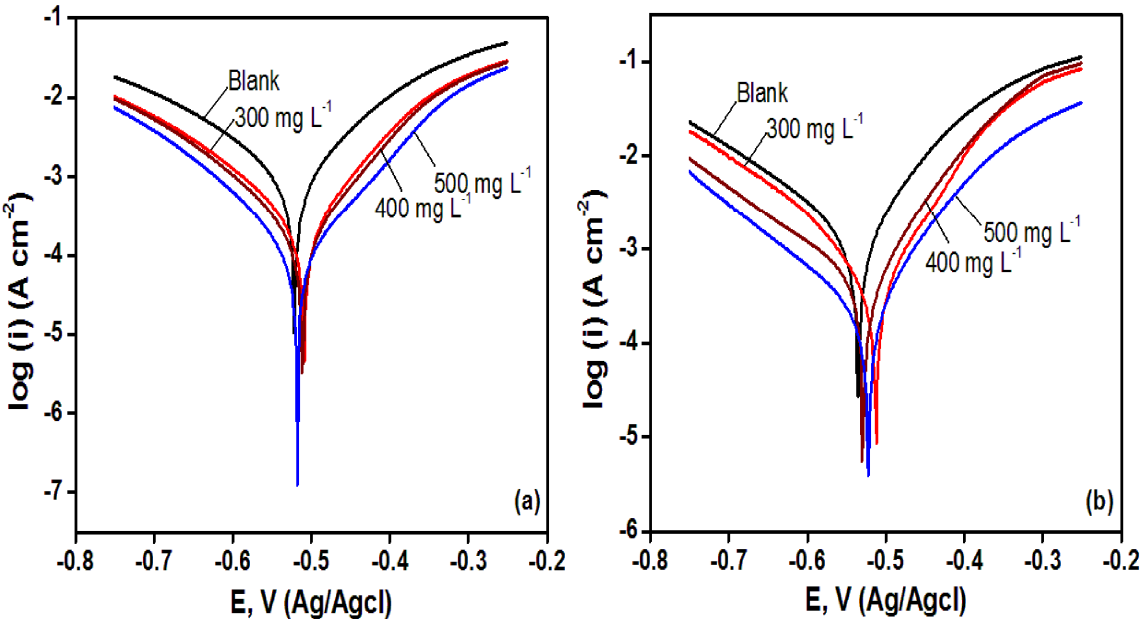

Figure 4.10 Tafel curve plot for mild steel in a) 1M HCl and b) 0.5 M H_2SO_4 with different concentrations of inhibitor at Room Temperature.

Table 4.3 Tafel polarization parameters obtained at different concentration of inhibitor for 1 M HCl and 0.5 M H_2SO_4 at RT.

Acid solution	Conc. (mg L^{-1})	-Ecorr (mV)	I corr (µA cm^{-2})	b_a (mV dec^{-1})	b_c (mV dec^{-1})	μ_p %	L_{PR} (Ω cm^2)
1 M HCl	Blank	521	1095	79	62	-	28
	300	508	255	103	74	77	96
	400	511	188	111	78	83	121
	500	517	102	113	84	91	200
0.5M H_2SO_4	Blank	534	1646	86	59	-	18
	300	511	479	121	81	71	45
	400	529	394	109	61	76	64
	500	521	265	101	65	84	99

From Table 9 it is evident that corrosion current density values remarkably decreased with increase in CBRE concentration. A maximum inhibition efficiency of 91% and 84 % was acknowledged in 1 M HCl and 0.5 M H_2SO_4 respectively at 500 mg L^{-1} concentration of the extract. In both acid media, equilibrium corrosion potential (E_{corr}) showed a shift with respect to blank solutions in presence of inhibitor; however, the shift did not follow any pattern. Also, the difference of E_{corr} of inhibited (500 mg L^{-1}) and uninhibited mild steel was not more than 85 mV. These facts indicated that CBRE inhibited mild steel corrosion by working in a mixed type inhibition mode [Ferreira et al., 2004; Li et al., 2008]. In addition, it was noticed that the change of slope values (b_a and

b_c) were also not in a particular direction, which highlighted the same fact as mentioned above, i.e., CBRE was a mixed type inhibitor. The reason of effective corrosion inhibition by the extract could be explained on the basis of polarization resistance values of mild steel obtained in presence of inhibitor (Table 9). In 1 M HCl and 0.5 M H_2SO_4, the resistance was 28 Ω cm^2 and 18 Ω cm^2 respectively. On addition of inhibitor, polarization resistance significantly increased and attained a maximum value of 200 Ω cm^2 and 99 Ω cm^2 at 500 mg L^{-1} inhibitor concentration in HCl and H_2SO_4 respectively. Possibly, organic moieties of the extract accumulated at metal-acid interface and restrained further corrosion of the mild steel [Godec and Dolecek, 2004]. This assumption could be supported by increasing polarization resistance values with the extract concentration. On a whole, it could be concluded on the basis of Tafel polarization study that CBRE acted as a mixed type inhibitor in both acid solutions and inhibited mild steel corrosion by suppressing both anodic and cathodic reactions.

4.4 Electrochemical Impedance Spectroscopy

Response of mild steel to alternating current in 1 M HCl and 0.5 M H_2SO_4 with and without inhibitor are shown in Figure 37. It is evident from Figure 37 that impedance spectra demonstrated single capacitive loop (one time constant) in both acid solutions, suggesting that CBRE performed inhibitory action via reducing charge transfer reactions at metal acid interface.

Careful inspection of Figure 37a and b revealed that the shape of Nyquist plots did not change with the extract concentration, suggesting that the corrosion inhibition mechanism was not affected by addition of inhibitor. Further investigation of the results provided that

Nyquist plots were not exact semi circles but depressed semi circles. This behavior of mild steel electrode is often observed due to heterogeneity and irregularity of the metal surface, which arises from surface roughness or random adsorption of the inhibitor molecules over metal surface [Fawcett et al. 1992, Li et al, 2014].

From analysis of impedance spectra it was evident that diameters of semi circles increased with increase in inhibitor concentration, indicating that charge transfer resistance of mild steel were increasing with the inhibitor concentration. The values of frequency at the point of the highest imaginary impedance (indicated by an arrow) are shown in Figure 37a and b. It could be observed via Nyquist plots that the frequency value was decreasing with the extract concentration, which showed the increase in charge transfer resistance with increase in inhibitor concentration. In addition, it was analyzed from bode plots that phase angle magnitude increased as a function of CBRE amount (Figure 37 c and d). This observation suggested that surface conditions of electrode improved with the addition of inhibitor and showed enhanced capacitive behavior [Lebrini et al., 2005; Yadav et al, 2013] .

An electrochemical circuit was shown with the EIS results (Figure 37e), which was used to simulate experimental results. In this circuit R_s belongs to solution resistance, R_t is charge transfer resistance and CPE denotes a constant phase element. The impedance function of the CPE can be explained by the equation 23. Through analysis of equation 23 it is obvious that the CPE will show the characteristic of a resistive circuit if n=0 (Y= 1/R), capacitive circuit if n= 1 (Y= C) and inductive circuit if n=-1 (Y=1/L) [J.R. Macdonald, 1987]. The electrochemical parameters of corrosion like R_s, R_t, C_{dl}, Y_0, and n were determined by ZSimDemo (version 3.22 d) software and listed in Table 10.

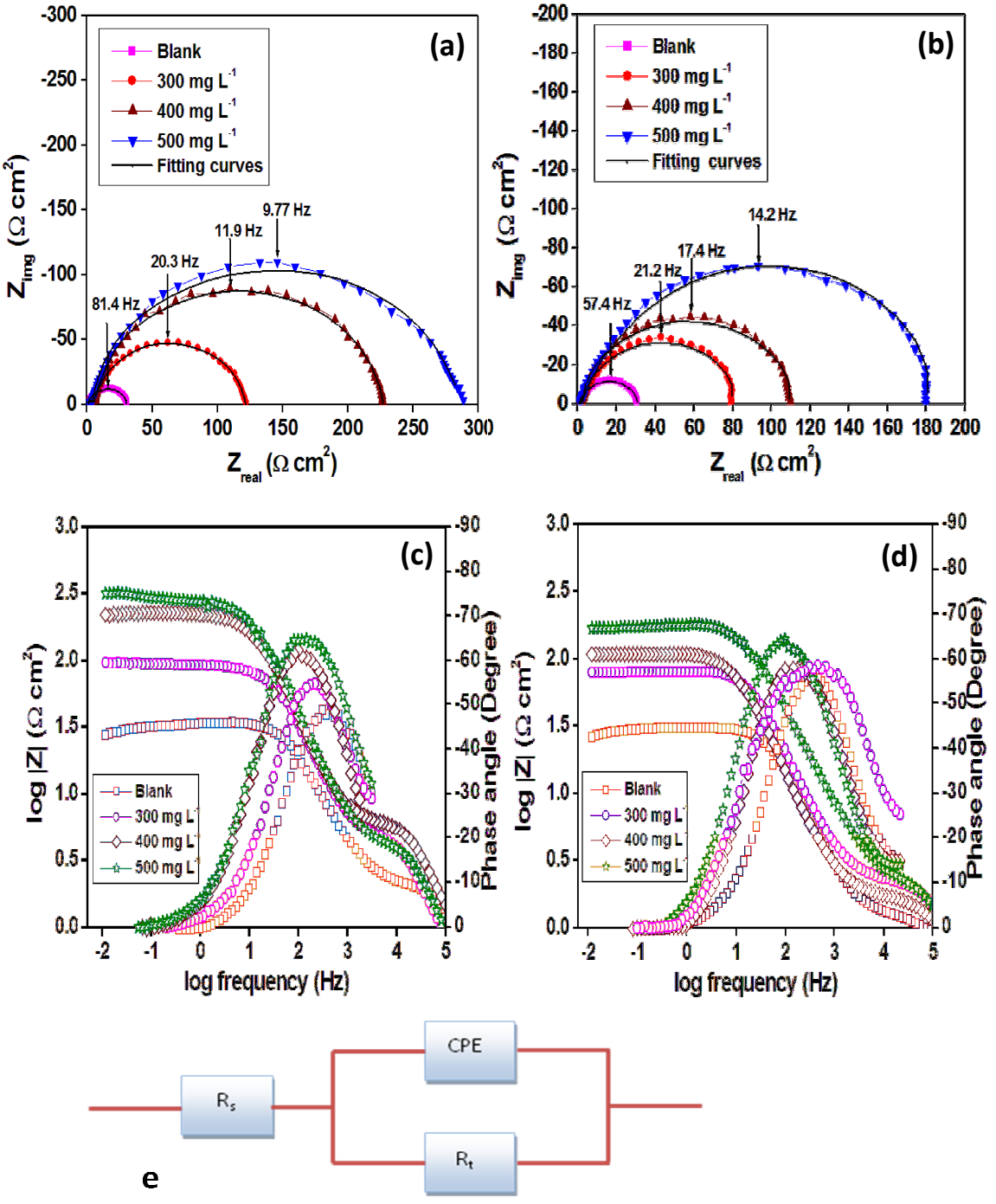

Figure 4.11 Showing Nyquist plots for mild steel in (a) 1 M HCl , (b) 0.5 M H_2SO_4 and bode plots in (c) 1 M HCl, (d) 0.5 M H_2SO_4 at different concentrations of CBRE at room temperature. (e) Equivalent electrochemical circuit for fitting of experimental results.

Table 4.4 Impedance parameters for mild steel in 1 M HCl and 0.5 M H_2SO_4 in absence and presence of different concentrations of inhibitor at RT

Acid solution	Conc. (mg L^{-1})	R_s (Ω cm^2)	R_t (Ω cm^2)	n	Y_0 ($10^{-6}\Omega^{-1}cm^{-2}$)	C_{dl} (μF cm^{-2})	μ_{Rt} %
1 M HCl	Blank	1.03	32	0.802	147.00	41.70	-
	300	0.82	122	0.816	102.40	37.80	76
	400	1.92	225	0.825	80.45	34.12	87
	500	0.65	287	0.832	64.30	28.60	90
0.5 M H_2SO_4	Blank	1.16	27	0.820	164.80	49.90	-
	300	1.23	79	0.831	126.00	39.30	66
	400	1.30	109	0.839	89.00	36.80	82
	500	1.25	179	0.840	81.20	35.96	85

Through investigation of Table 10 it was revealed that charge transfer resistance values increased with the extract concentration in both acid solutions. The increase in R_t values could be attributed to molecular adsorption of inhibitor at most active sites on the metal surface, which reduced surface heterogeneity (reflected in n values) as well as blanketed the surface [Lebrini et al., 2007, Ostovari et al., 2009]. This fact could be explained further by the equation 25.

On the basis of Helmholtz equation, it can be stated that increase in double layer capacitance will cause either increase in local dielectric constant or decrease in thickness of inhibitive layer, or both. In the view of above statement, decrease in C_{dl} values (Table

10) with the inhibitor concentration could be related with thickness of protective film (increase in R_t values) and hence better corrosion inhibition achieved.

4.5 Surface Morphology Analysis

Figure 38 illustrates surface morphology of test samples immersed in HCl and H_2SO_4 solutions alone and in presence of maximum concentration of CBRE. Before performing the experiment, mild steel sample was abraded by emery paper. Due to polishing effect, some scratches were generated on the metal surface and could be clearly observed in Figure 38a. When test samples were immersed in acid, a violent reaction took place and heavy damage of mild steel occurred. Acid solutions caused drastic change in morphology of steel, which could be noticed in Figure 38 b and d. However, it was observed that H_2SO_4 damaged mild steel more violently than HCl. On the other side, drastic improvement in surface texture of the samples was seen in presence of CBRE (Figure 38 c and e).

The similar information was obtained by AFM study (Figure 39), i.e., better surface texture in comparison to the surface texture of corroded mild steel in acid solutions alone. The surface roughness of mild steel specimen was found as 26 nm while roughness in HCl and H_2SO_4 was recorded as 118 nm and 165 nm respectively. In presence of CBRE, the surface roughness was 39 nm (HCl) and 89 nm (H_2SO_4). Thus, it was obvious from AFM study that CBRE retarded the effect of acid solutions and effectively maintained the surface regularity.

Thus, on the basis of surface morphology study it could be stated that the extract successfully inhibited mild steel corrosion in acid solutions. However, the effect was

more prominent in 1 M HCl than 0.5 M H_2SO_4.

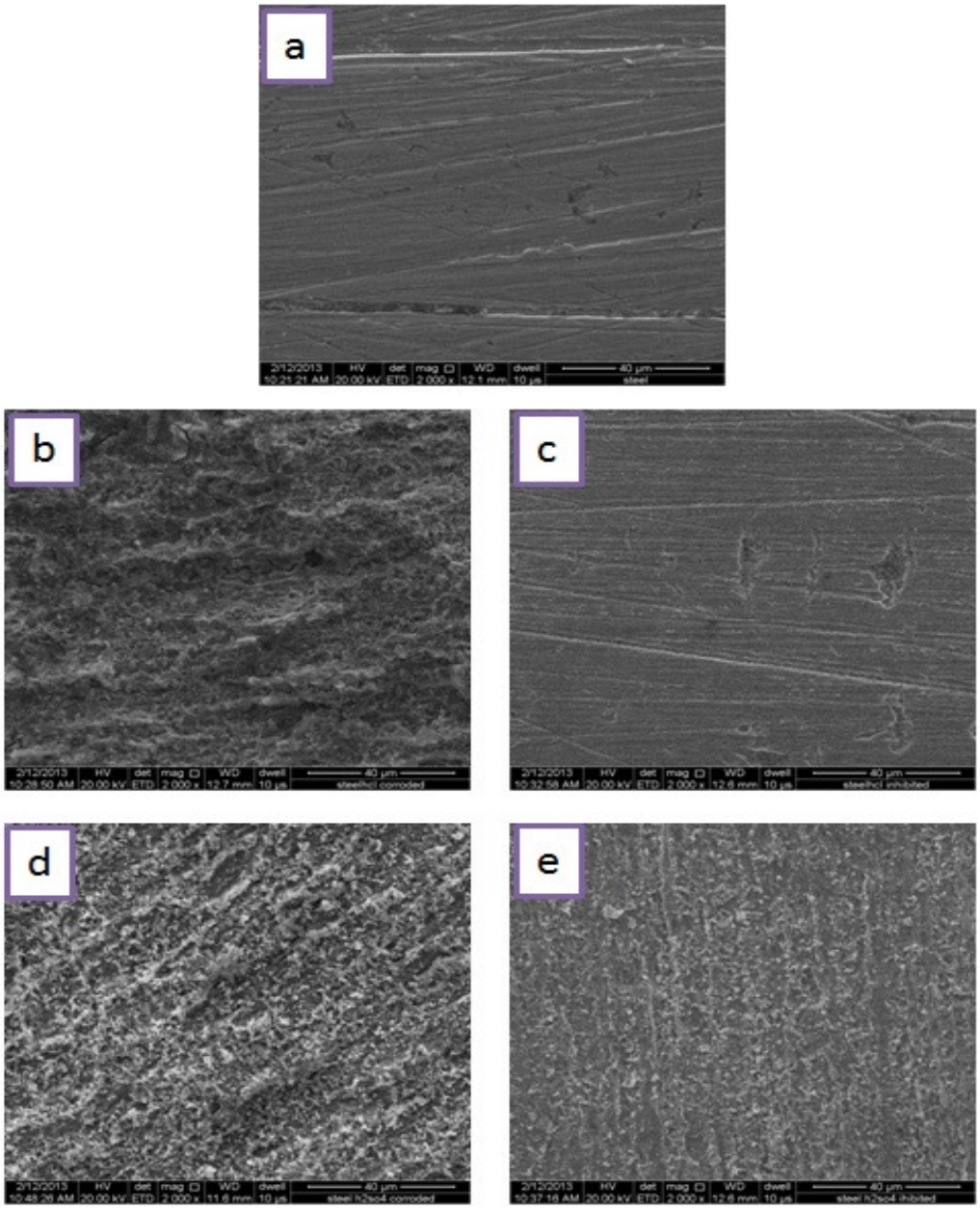

Figure 4.12 SEM images showing surface morphology of (a) mild steel test sample before immersion, (b) after immersion in 1 M HCl, (c) in presence of inhibitor (500 mg L^{-1}) in 1 M HCl, (d) after corrosion in 0.5 M H_2SO_4 (e) in presence of inhibitor (500 mg L^{-1}) in 0.5 M H_2SO_4

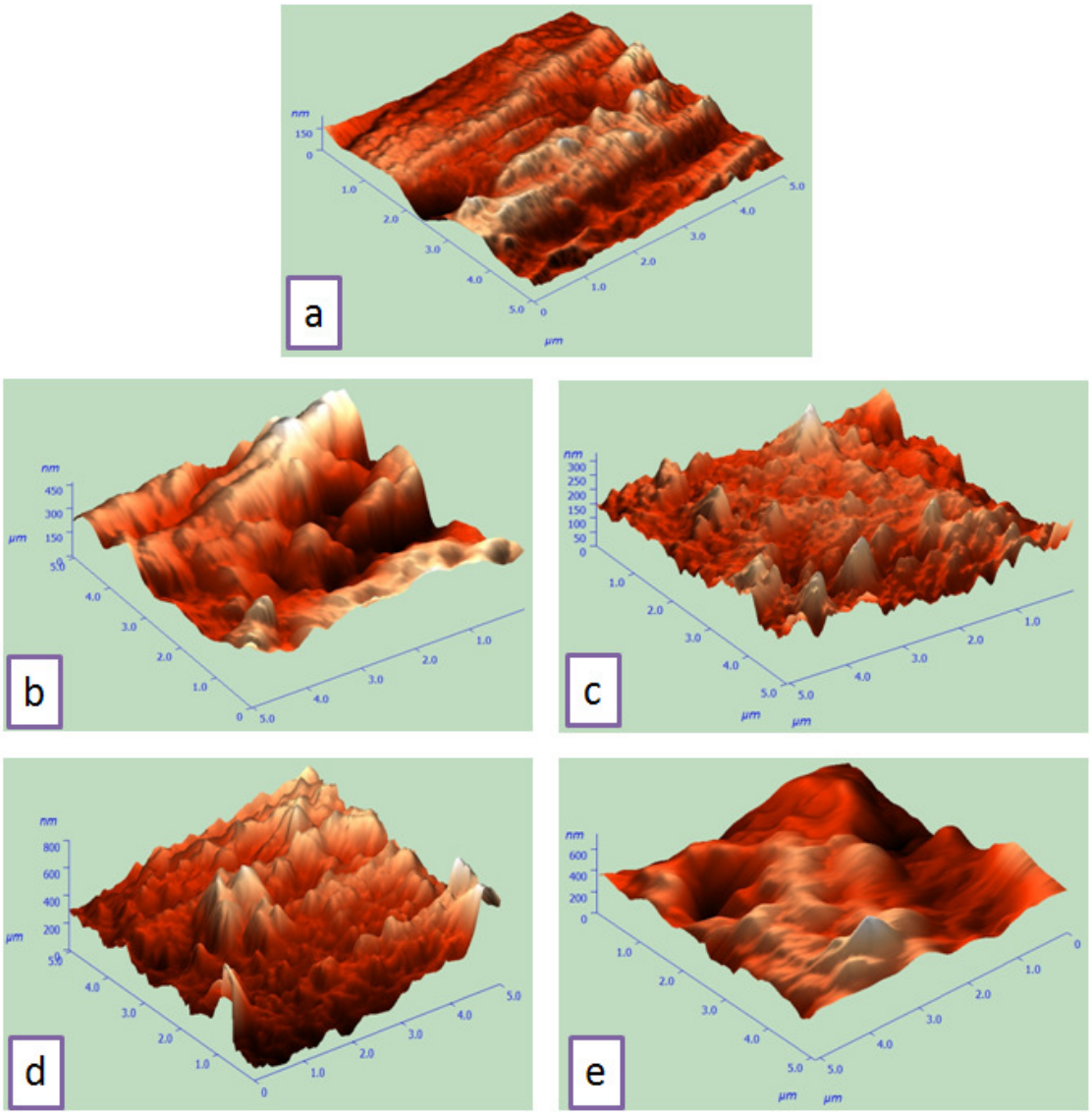

Figure 4.13 3D AFM images showing morphology of (a) mild steel sample, (b) corroded surface in 1 M HCl, (c) inhibited surface (500 mg L^{-1}) in 1 M HCl, (d) corroded in 0.5 M H_2SO_4 and (e) inhibited (500 mg L^{-1}) in 0.5 M H_2SO_4

4.6 Corrosion Inhibition Mechanism

It was known via characterization results of the extract that CBRE was having various organic compounds. Among all the chemical constituents, saponins (furostanol saponins, FTIR) were a major compound [Deore et al, 2010]. Saponins are described as secondary

metabolite compounds, which contain benzene rings, hetero (N, O) atoms along with -OH functional group in their chemical structure (Figure 40). The other organic compounds of the extract, such as, tannins and flavanoids, are abundant in aromatic rings and hetero cycles. Hence, it is worth to mention here that inhibitive property of the extract belong to successful adsorption of these molecules.

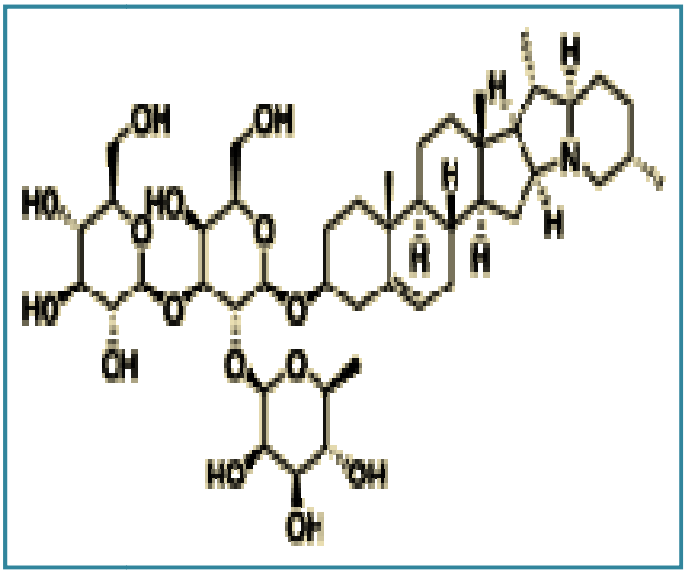

Figure 4.14 Showing general chemical structure of Saponins

The organic moieties can be adsorbed on metal surface through (a) Physical adsorption, (b) Chemical adsorption, or (c) mixed type adsorption [Obot et al.; 2010, Singh et al., 2013]. In acidic environments, the acid anions (chloride ions/sulphate ions) first adsorb on metal surface and then create favorable conditions for adsorption of positively charged inhibitor molecules on metals. Probably, CBRE molecules (protonated form) adsorbed on mild steel by the mechanism as stated above and formed an inhibitive layer at metal-acid interface [Benali et. al., 2014; Singh et al., 2014]. It was also possible that the protective layer on mild steel surface was formed via chemical bonding between pi electrons or lone pair electrons of the extract molecules and vacant d-orbit electrons of iron. Additionally,

organic matters of CBRE might interact with Fe^{2+} and produce iron-inhibitor complex compounds. These chemicals could be adsorbed on mild steel via a weak chemical bond [Mistry et al., 2011]. Thus, it was evident that corrosion inhibition of mild steel was acknowledged due to adsorption of CBRE constituents over mild steel surface, which was also supported by the results of different techniques and SEM images. However, an exact method of adsorption could not be envisaged due to unknown molecular weight of the extract. Furthermore, it was found through corrosion study that CBRE was more effective in HCl than H_2SO_4. The reason of this fact could be explained on the basis of degree of hydration. Chloride ions have smaller degree of hydration in comparison to sulphate ions, which created more favorable conditions for adsorption of CBRE molecules on mild steel surface.